iScience

CellPress
OPEN ACCESS

Article

Spatio-temporal requirements of Aurora kinase A in mouse oocyte meiotic spindle building

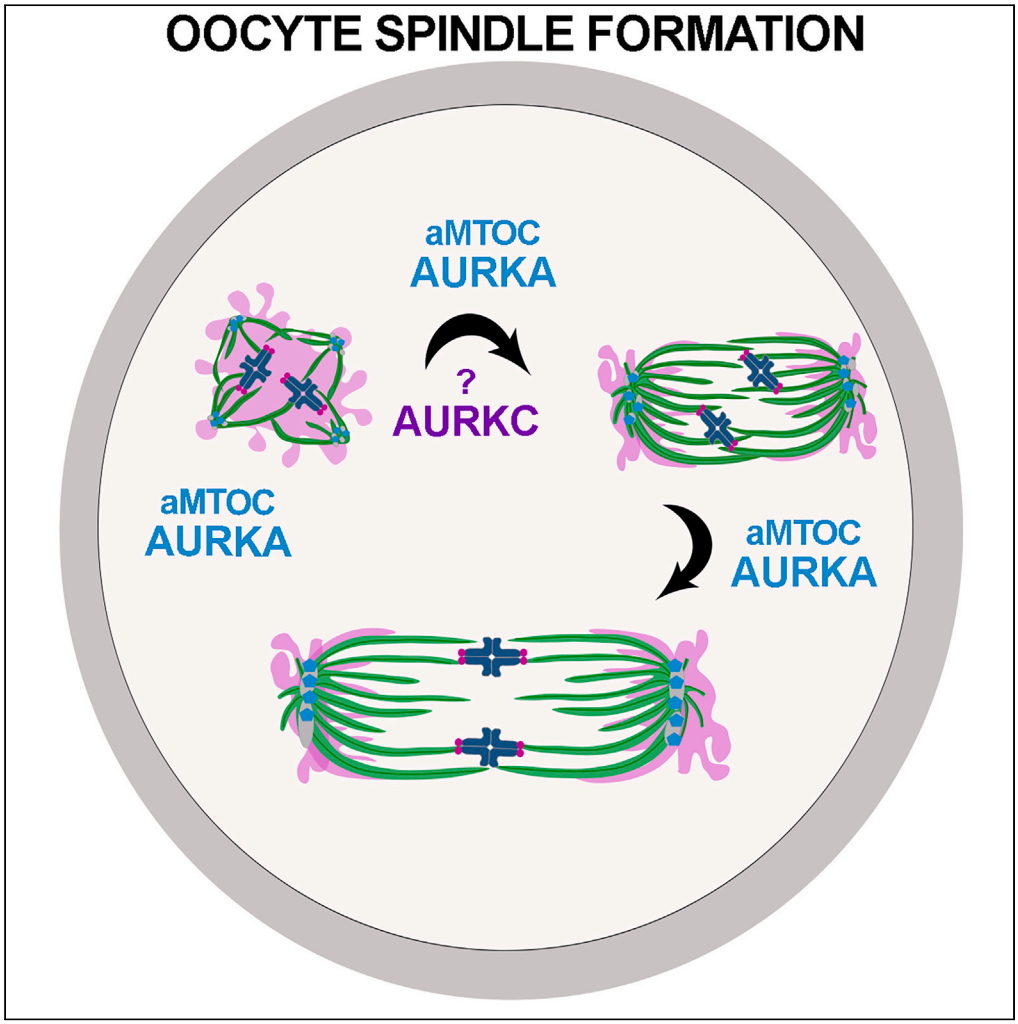

Cecilia S. Blengini, Michaela Vaskovicova, Jan Schier, David Drutovic, Karen Schindler

cb928@hginj.rutgers.edu (C.S.B.)
ks804@hginj.rutgers.edu (K.S.)

Highlights

High-resolution analyses of AURKA requirements during oocyte spindle assembly

AURKA is required in early spindle assembly and later for spindle stability

AURKC is required in late pro-metaphase for spindle bipolarization

AURKA spindle pole controls meiotic spindle building and stability

Blengini et al., iScience 27, 110451
August 16, 2024
https://doi.org/10.1016/j.isci.2024.110451

iScience

CellPress
OPEN ACCESS

Article

Spatio-temporal requirements of Aurora kinase A in mouse oocyte meiotic spindle building

Cecilia S. Blengini,[1,2,6,*] Michaela Vaskovicova,[3,4,6] Jan Schier,[5] David Drutovic,[3] and Karen Schindler[1,2,7,*]

SUMMARY

Meiotic spindles are critical to ensure chromosome segregation during gamete formation. Oocytes lack centrosomes and use alternative microtubule-nucleation mechanisms for spindle building. How these mechanisms are regulated is still unknown. Aurora kinase A (AURKA) is essential for mouse oocyte meiosis because in pro-metaphase I it triggers microtubule organizing-center fragmentation and its expression compensates for the loss of the two other Aurora kinases (AURKB/AURKC). Although knockout mouse models were useful for foundational studies, AURK spatial and temporal functions are not yet resolved. We provide high-resolution analyses of AURKA/AURKC requirements during meiotic spindle-building and identify the subcellular populations that carry out these functions: 1) AURKA is required in early spindle assembly and later for spindle stability, whereas 2) AURKC is required in late pro-metaphase, and 3) Targeted AURKA constructs expressed in triple AURK knockout oocytes reveal that spindle pole-localized AURKA is the most important population controlling spindle building and stability mechanisms.

INTRODUCTION

In humans, oocyte aneuploidy is the leading cause of early miscarriage. Spindles are critical for ensuring euploidy and spindle mechanics are frequently faulty in human oocytes.[1] After losing their centrioles during development,[2,3] oocytes must use alternative mechanisms to form bipolar spindles during meiosis. For example, mouse oocytes rely on two mechanisms: the Ran-GTP pathway[4–7] and acentriolar microtubule organizing centers (aMTOCs).[5,8,9] The Ran-GTP pathway generates a gradient of spindle assembly factors emanating from chromatin to control microtubule (MT) polymerization.[6,10] aMTOCs are structures composed of pericentriolar material that nucleate microtubules.[8] Notably, not all organisms have aMTOCs in their oocytes, such as human[4] and Drosophila.[11] During mouse oocyte meiotic maturation, aMTOCs undergo a series of structural changes. First, upon nuclear envelope breakdown (NEBD), aMTOCs fragment. Then, these fragments sort and separate on either side of chromosomes and cluster together to form two spindle poles.[12] How these processes are regulated is still not fully understood. In mouse oocytes, both mechanisms of MT nucleation are present and contribute to spindle formation during meiosis I and II.[6,7,9,12] On the other hand, Ran-GTP may be the main pathway for human oocyte MT nucleation.[4] However, recent evidence shows that some components of the aMTOC pathway (γ-tubulin, Numa), although they do not form a defined aMTOC structures as mouse oocytes do, are enriched at spindle poles and contribute to the morphological phenotype of spindle poles.[1] Furthermore, genetic variants of some centrosome/aMTOC components are associated with high rates of embryo aneuploidy in women undergoing *in vitro* fertilization.[13] Finally, a third mechanism of MT-nucleation from kinetochores (KT) exists in human oocytes. This mechanism involves a structure named human oocyte MTOC (huoMTOC), which fragments upon NEBD and the fragments localize at KTs and nucleate MTs.[14] Interestingly, one of the major components of huoMTOCs is TACC3, a liquid-like spindle domain (LISD) component recently described in mouse oocytes.[14,15] LISDs ensure that microtubule-regulating proteins are concentrated near the meiotic spindle, but this domain has not been detected in human oocytes. Therefore, the significance of an MTOC-like pathway in human oocytes is not fully understood.

The Aurora protein kinases (AURK) have been extensively studied for the roles they play in regulating accurate chromosome segregation in mitosis and meiosis. The mammalian genome encodes three members: Aurora kinase A (AURKA), Aurora kinase B (AURKB), and Aurora kinase C (AURKC). In mouse oocytes, each isoform has a specific subcellular localization. AURKA concentrates at aMTOCs,[16,17] and also has a minor chromosomal population.[18] AURKB is mainly cytoplasmic and around the spindle, and AURKC is localized at the interchromatid axis of meiosis I bivalents, at KTs, and at spindle poles.[19] Through mouse knockout studies, we found that although each isoform is important for female fertility and oocyte meiosis, only AURKA is essential for fertility.[20,21] Female mice lacking AURKC are subfertile with oocytes having mild chromosome alignment defects at metaphase I.[22] Furthermore, when AURKC was inhibited by the expression of a dominant-negative

[1]Department of Genetics, Rutgers, The State University of New Jersey, New Brunswick, NJ 08901, USA
[2]Human Genetics Institute of New Jersey, Piscataway, NJ 08854, USA
[3]Laboratory of DNA Integrity, Institute of Animal Physiology and Genetics of the Czech Academy of Sciences, Libechov, Czech Republic
[4]Department of Cell Biology, Faculty of Science, Charles University, Prague, Czech Republic
[5]The Czech Academy of Sciences, Institute of Information Theory and Automation, Piscataway, NJ 08854, USA
[6]These authors contribute equally
[7]Lead contact
*Correspondence: cb928@hginj.rutgers.edu (C.S.B.), ks804@hginj.rutgers.edu (K.S.)
https://doi.org/10.1016/j.isci.2024.110451

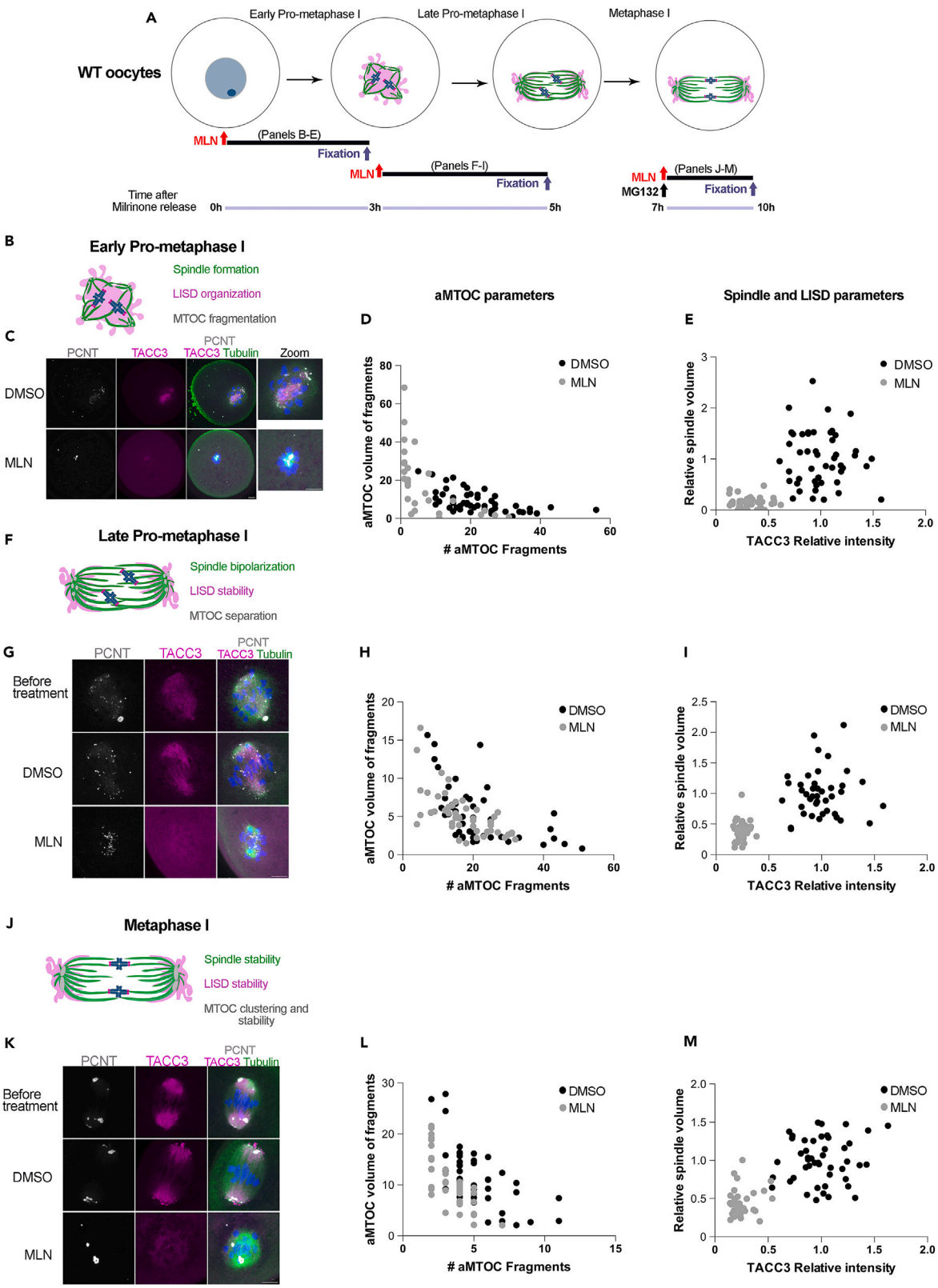
A
Early Pro-metaphase I
Late Pro-metaphase I
Metaphase I
WT oocytes
MLN
(Panels B-E)
Fixation
MLN
(Panels F-I)
Fixation
MLN
MG132
(Panels J-M)
Fixation
Time after Milrinone release
0h
3h
5h
7h
10h
B
Early Pro-metaphase I
Spindle formation
LISD organization
MTOC fragmentation
C
PCNT
TACC3
PCNT TACC3 Tubulin
Zoom
DMSO
MLN
aMTOC parameters
Spindle and LISD parameters
D
aMTOC volume of fragments
aMTOC Fragments
DMSO
MLN
E
Relative spindle volume
TACC3 Relative intensity
DMSO
MLN
F
Late Pro-metaphase I
Spindle bipolarization
LISD stability
MTOC separation
G
PCNT
TACC3
PCNT TACC3 Tubulin
Before treatment
DMSO
MLN
H
aMTOC volume of fragments
aMTOC Fragments
DMSO
MLN
I
Relative spindle volume
TACC3 Relative intensity
DMSO
MLN
J
Metaphase I
Spindle stability
LISD stability
MTOC clustering and stability
K
PCNT
TACC3
PCNT TACC3 Tubulin
Before treatment
DMSO
MLN
L
aMTOC volume of fragments
aMTOC Fragments
DMSO
MLN
M
Relative spindle volume
TACC3 Relative intensity
DMSO
MLN

Figure 1. AURKA is required at early pro-metaphase I and metaphase I for spindle building

(A) Experimental design of WT oocytes treated with MLN during oocyte maturation. Red arrows indicate MLN addition time; blue arrows indicate fixation time.

(B, F, J) Schematic of spindles at indicated stages, and the processes analyzed.

(C, G, K) Representative confocal images of oocytes fixed at the indicated stages with and without MLN, immunostained with PCNT (gray), TACC3 (magenta), Tubulin (green) and DAPI (blue). Scale bars 10 μm.

(D, H, L) Quantification of aMTOC parameters in (A), (G), (K) respectively.

(E, I, M) Quantification of spindle and LISD parameters in (A), (G), (K) respectively. Black dots: DMSO-treated; gray dots: MLN- treated. See also Figure S1 which contains statistics.

mutant, oocytes failed to become bipolar.[19] Females in which AURKB was specifically deleted in oocytes exhibited premature age-related infertility,[21] characterized by an increase in meiosis II aneuploidy caused by a reduction in the expression of spindle assembly checkpoint (SAC) proteins. Females that lack AURKB and AURKC (BC-knockout; KO), in which oocytes contain only AURKA, are fertile. In these oocytes, AURKA increases its population on chromosomes, compensating for the loss of AURKB/C.[21] In contrast, in oocyte-specific *Aurka* knockout mice, females are sterile, and their oocytes arrest at metaphase I with unfragmented aMTOCs and a disorganized TACC3-dependent spindle domain, a marker of the LISD.[15] As a result, these oocytes have small, abnormal spindles.[20] This phenotype is consistent with previous reports in which AURKA was inhibited by a small molecule inhibitor in oocytes.[15,23,24] Because aMTOC fragmentation is the first step of spindle assembly, it is unclear whether AURKA is required for later spindle formation steps, and which localized AURK population is essential for spindle formation. Here, we aimed to evaluate the spatial and temporal requirements of AURKA during meiotic maturation in mouse oocytes.

RESULTS AND DISCUSSION

Aurora kinase A is required for multiple steps of meiotic spindle formation

To temporally resolve specific AURKA requirements in oocyte meiosis, we inhibited AURKA with MLN8237 (MLN) in WT oocytes. The concentration of MLN chosen was previously determined as AURKA specific, not reducing AURKC activity.[25] We focused on determining AURKA functions in three critical spindle formation steps: early pro-metaphase I, late pro-metaphase I and metaphase I (Figure 1A). Each group was immunostained with Pericentrin (Pcnt), TACC3, and α-tubulin antibodies to visualize aMTOCs, LISD, and spindles, respectively. We excluded oocytes that did not resume meiosis from the analysis. We evaluated changes in aMTOC numbers and volume, TACC3 intensity, and spindle volume. When inhibiting late pro-metaphase and metaphase steps, we examined oocytes prior to MLN addition to ensure that the earlier processes had occurred normally.

First, we evaluated early pro-metaphase I (Figure 1B), and observed that MLN-treated oocytes had fewer aMTOCs, which were larger in volume than aMTOCs in control oocytes, consistent with fragmentation failure described in *Aurka* KO oocytes[20] (Figures 1C, 1D, S1A, and S1B). Furthermore, spindle volume and TACC3 intensity measurements revealed two distinct clusters: MLN-treated oocytes had smaller spindles and reduced TACC3 intensity compared to controls (Figures 1C, 1E, S1C, and S1D). These results are also consistent with our previous data in *Aurka* KO oocytes.[20] In contrast, when AURKA was inhibited at late pro-metaphase I (Figures 1A and 1F), we also observed a reduction in aMTOC number; however, the volume was not altered compared to controls (Figures 1G, 1H, S1E, and S1F). Similar to early inhibition, spindle volume and TACC3 intensity were different. Oocytes exposed to MLN produced smaller spindles (~55% reduction) with reduced TACC3 intensity compared to controls (Figures 1G, 1I, S1G, and S1H), suggesting that AURKA is essential to maintain LISD stability and achieve full spindle length.

Finally, we evaluated metaphase I spindle stability (Figures 1A and 1J) by inhibiting AURKA after bipolar spindles formed and oocytes had reached metaphase I. Again, the data clustered into two groups. MLN-treated oocytes had fewer aMTOCs (Figures 1K, 1L, S1I, and S1J) compared to controls, and they had a significant reduction in both spindle volume and TACC3 intensity (Figures 1K, 1M, S1K, and S1L). These results are consistent with previous studies where spindle pole structure was altered upon AURKA inhibition causing spindle defects.[20,24] Taken together, these data indicate that AURKA plays a critical role in several steps during the spindle formation process. First, AURKA controls aMTOC fragmentation and LISD organization. Next, AURKA maintains LISD stability and spindle length, and finally, AURKA is required for spindle stability possibly by maintaining LISD organization.

AURKA and AURKC genetically interact to control spindle building,[21] but which critical steps they function in are unclear. To fully understand how AURKA and AURKC participate in spindle building, we treated BC-KO (AURKA only) oocytes with MLN at the same time points in spindle assembly (Figure 2A) and then compared these changes to the changes we observed in WT oocytes (Figure 1). When evaluating early pro-metaphase I and metaphase I spindles, we did not observe differences in the response of BC-KO compared to WT oocytes treated with MLN (Figures 2B–2E, 2J–2M, S2A–S2D, and S2I–S2L). However, when we examined late pro-metaphase I (Figure 2F), MLN-inhibited BC-KO oocytes behaved differently from WT. BC-KO oocytes treated with MLN had over-clustered aMTOCs, characterized by fewer fragments with greater volume than in controls (Figures 2G, 2H, S2E, and S2F). Moreover, the TACC3 domains were also disorganized, and the spindle volume was reduced by 70%, compared to 55% in WT oocytes (Figures 2G, 2I, S2G, and S2H). These differences between WT and BC-KO oocytes suggest a role for AURKC to separate aMTOCs during late-prometaphase I, a function that requires further investigation.

We observed different responses to AURKA inhibition between WT and BC-KOs. To refine the temporal order in spindle assembly, we acutely treated early pro-metaphase I oocytes with MLN and performed live-cell imaging using light sheet microscopy. Prior to adding

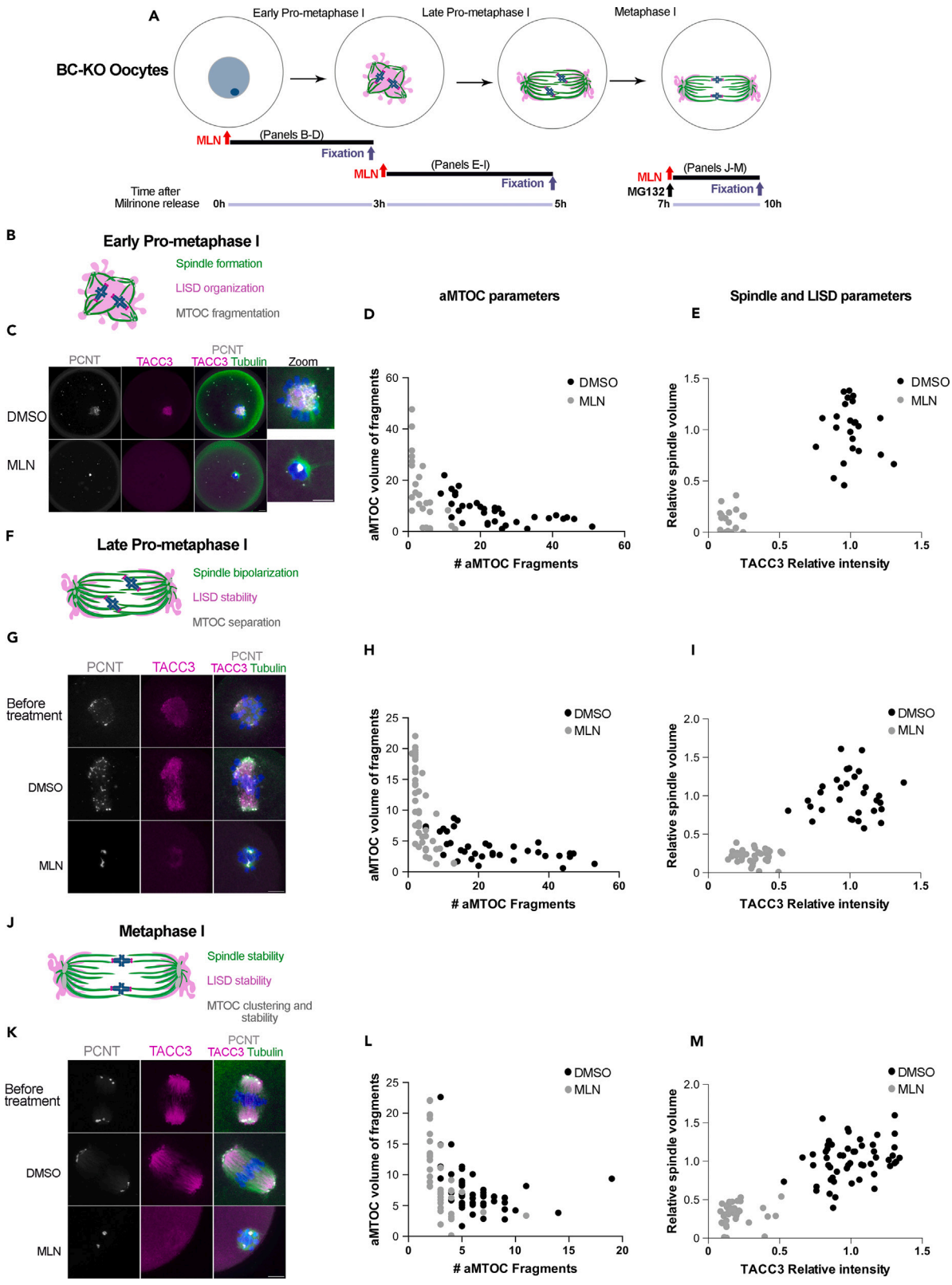
A
Early Pro-metaphase I
Late Pro-metaphase I
Metaphase I
BC-KO Oocytes
MLN
(Panels B-D)
Fixation
MLN
(Panels E-I)
Fixation
MLN
(Panels J-M)
MG132
Fixation
Time after Milrinone release
0h
3h
5h
7h
10h
B
Early Pro-metaphase I
Spindle formation
LISD organization
MTOC fragmentation
C
PCNT
TACC3
PCNT TACC3 Tubulin
Zoom
DMSO
MLN
aMTOC parameters
Spindle and LISD parameters
D
E
aMTOC volume of fragments
aMTOC Fragments
Relative spindle volume
TACC3 Relative intensity
DMSO
MLN
F
Late Pro-metaphase I
Spindle bipolarization
LISD stability
MTOC separation
G
Before treatment
H
I
J
Metaphase I
Spindle stability
LISD stability
MTOC clustering and stability
K
L
M

Figure 2. AURKC is required at late pro-metaphase I for aMTOC separation

(A) Experimental design of BC-KO oocytes treated with MLN; Red arrows indicate MLN addition time; blue arrows indicate fixation time.

(B, F, J) Schematic of spindles at the indicated stages, and the processes analyzed.

(C, G, K) Representative confocal images of oocytes fixed at the indicated stages with and without MLN, immunostained with PCNT (gray), TACC3 (magenta), Tubulin (green) and DAPI (blue). Scale bars 10 μm.

(D, H, L) Quantification of aMTOC parameters in (A), (G), (K), respectively.

(E, I, M) Quantification of spindle and LISD parameters in (A), (G), (K), respectively. Black dots: DMSO- treated; gray dots: MLN-treated. See also Figure S2 which contains statistics.

MLN, we observed an increase in spindle volume and an increase in aMTOC number in both WT (n = 27/27) and BC-KO oocytes (n = 15/15) (Video S1). Compared to controls, after MLN addition in both WT and BC-KO oocytes, spindle volume rapidly reduced (10 min) (n = 16/16 of MLN-treated WT oocytes, n = 9/9 of MLN-treated BC-KO oocytes) (Figures 3A, 3B, and 3D). Notably, 56% of BC-KO (5/9 oocytes) oocytes lost their spindles after 8 h of maturation, a phenotype not observed in WT MLN-treated oocytes (Video S1). The behavior of aMTOCs was also altered. Both WT and BC-KO MLN-treated oocytes had fewer aMTOCs that were slightly larger (Figures 3A, 3C, and 3E). In BC-KO oocytes, aMTOC reduction was greater compared to WT oocytes. These results suggest that AURKA is required in early spindle assembly steps and later for spindle stability, whereas AURKC is required in late pro-metaphase to regulate aMTOCs. One possibility is that AURKC has a role in sorting and clustering aMTOCs at late pro-metaphase I. Previous evidence showed that loss of AURKC activity in mouse oocytes causes defects in aMTOC clustering resulting in multipolar spindles.[19] However, BC-KO oocytes may be more susceptible to AURKA inhibition than WT, because the localized amounts of AURKA protein are now reduced in other subcellular localizations where AURKB/C once were and less able to compensate.[21] In these studies, we did not assess a role for AURKB in spindle assembly. We focused on the role of AURKA and AURKC on spindle formation because these two isoforms localize at spindle poles, and AURKB does not. Our previous studies, and studies from others, showed that when AURKA is deleted or inhibited, oocytes cannot build a normal spindle.[20,15,23,24] Another reason that we did not evaluate AURKB, is that our previous studies indicated that AURKB has a minimal, if any, role in spindle formation.[21] In oocytes where AURKB was deleted, spindle formation occurs at near normal levels and oocytes expressing only AURKB (AC- KO) phenocopy *Aurka* KO oocytes (data not shown).

Polar and chromosomal-targeted Aurora kinase A partially rescue spindle defects

Because AURKA localizes to aMTOCs and chromosomes, we asked which localized population is required for spindle building. To help answer this question, we generated a mouse strain where oocytes lacked all three AURKs (ABC-KO). This genetic background provides an empty AURK canvas to overexpress different subcellular targeted AURKA fusions without competition or compensation from the others. To confirm that these oocytes lacked all three AURKs, we measured localized AURK activity. In WT oocytes, pABC localized predominantly at spindle poles (active AURKA), and chromosomes (active AURKB/C). No pABC signal was detected in ABC-KO oocytes, consistent with the deletion of the three AURKs (Figures S3A and S3B). We used this model to investigate whether expression of WT-AURKA (aMTOC and chromosomes), CDK5RAP2-AURKA (MTOC-AURKA), or H2B-AURKA (Chromatin-AURKA) could rescue the spindle defects in ABC-KO oocytes at metaphase I (Figure 4A). First, we tested whether these targeted fusions were active by expressing them in ABC-KO oocytes. We observed phosphorylation of INCENP at chromosomes (Figures S4A and S4B) and CDC25B at aMTOCs (Figures S4C and S4D) indicating that these fusion proteins are active at their targeted subcellular localization.

We first asked if the expression of both targeted proteins could rescue spindle formation. Non-injected ABC-KO oocytes were used as a reference. ABC-KO oocytes had small spindle volumes and disorganized TACC3 (Figures 4B, 4C, S5A, and S5B). Upon WT-AURKA expression, oocytes were fully rescued, forming bipolar spindles and organized TACC3 (Figures 4B, 4C, S5A, and S5B). However, when MTOC-AURKA and Chromatin-AURKA were co-expressed, we observed a partial rescue phenotype (Figures 4B, 4C, S5A, and S5B). TACC3 intensity was largely restored in these oocytes, but spindle volumes were still reduced by ∼50% compared to controls (Figures 4B, 4C, S5A, and S5B).

To determine which AURKA-localized population was responsible for the partial rescue, we analyzed the same parameters when individual AURKA fusion proteins were expressed. We observed that oocytes expressing MTOC-AURKA or Chromatin-AURKA also showed intermediate phenotypes (Figures 4D–4G). When MTOC-AURKA was expressed, the aMTOC fragmentation defect was rescued, because aMTOCs were smaller (Figures 4E, 4F, S5C, and S5D), but they failed to organize into two defined spindle poles. Although bipolar, spindles were ∼50% smaller (Figures 4D, 4G, and S5E) and TACC3 organization was partially restored compared to controls (Figures 4E, 4G, and S5F). When Chromatin-AURKA was expressed, aMTOC fragmentation was also rescued (Figures 4E, 4F, S5C, and S5D), but aMTOCs did not separate to form two poles and these oocytes did not form bipolar spindles. Spindles were 60% smaller (Figures 4D, 4G, and S5E) and TACC3 intensity was 60% reduced compared to WT-AURKA injected controls (Figures 4E, 4G, and S5F).

We next assessed the kinetics of meiotic maturation and spindle formation in ABC-KO oocytes using live-cell imaging. Similar to *Aurka* KO oocytes,[20] ABC-KO oocytes formed monopolar or short bipolar spindles (Figure 4H; Video S2). We observed that microtubule nucleation onset and spindle bipolarization were significantly delayed (Figures 4H–4J). Spindle volume was reduced compared to WT (Figures 4H and 4K), but expression of each AURKA fusion rescued the timing of microtubule nucleation and spindle elongation (Figures 4H–4J). However, spindle volume was only partially rescued in MTOC- or Chromatin-AURKA expressing oocytes compared to controls (Figures 4H and 4K). Although expression of the AURKA fusions to rescue spindle phenotypes in ABC-KO oocytes was a powerful strategy, there are caveats.

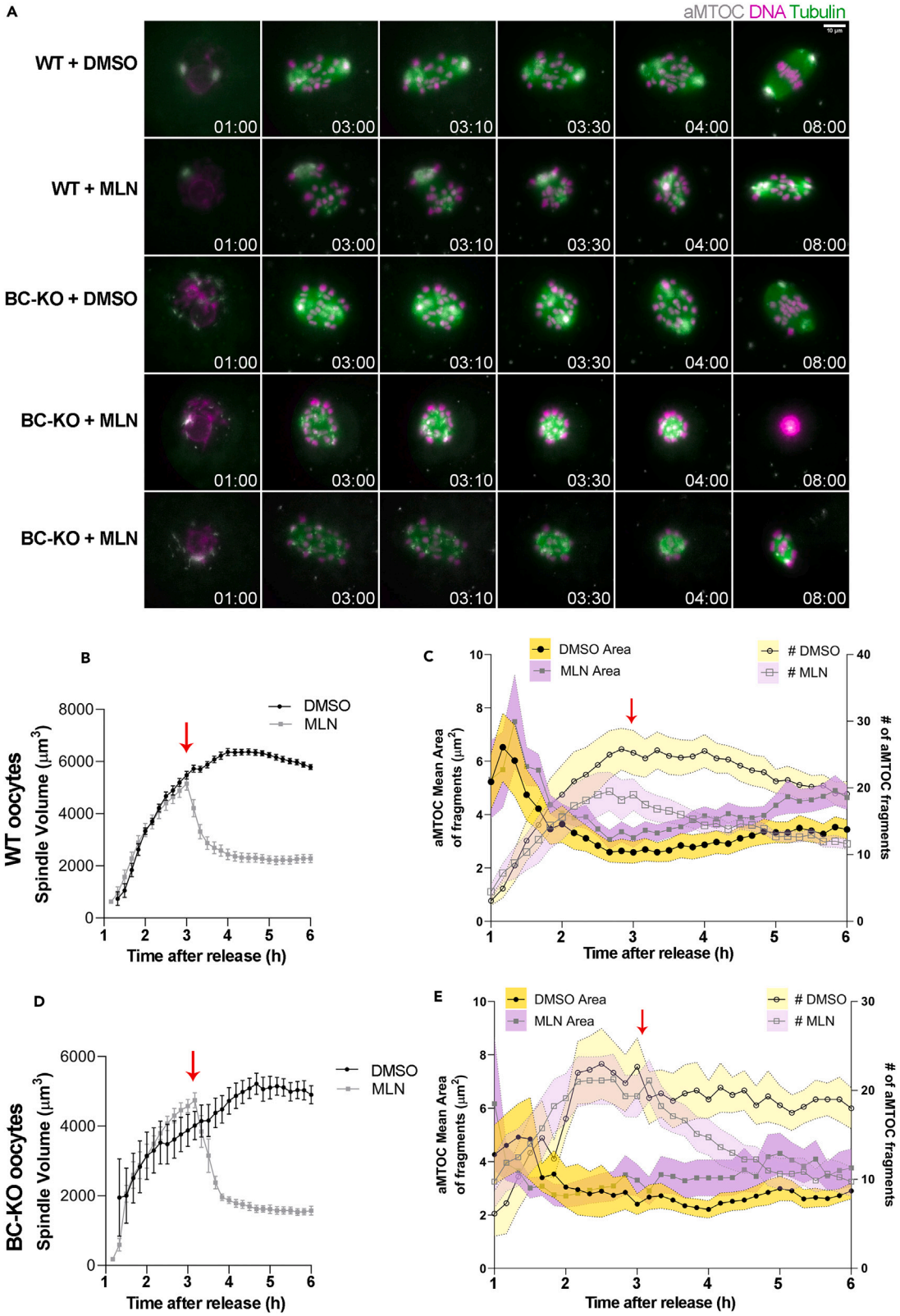
A
aMTOC DNA Tubulin
WT + DMSO
WT + MLN
BC-KO + DMSO
BC-KO + MLN
BC-KO + MLN
01:00
03:00
03:10
03:30
04:00
08:00
B
WT oocytes
Spindle Volume (μm3)
DMSO
MLN
Time after release (h)
C
DMSO Area
MLN Area
DMSO
MLN
aMTOC Mean Area of fragments (μm2)
# of aMTOC fragments
Time after release (h)
D
BC-KO oocytes
Spindle Volume (μm3)
DMSO
MLN
Time after release (h)
E
DMSO Area
MLN Area
DMSO
MLN
aMTOC Mean Area of fragments (μm2)
# of aMTOC fragments
Time after release (h)

Figure 3. AURKA and AURKC specific functions at late pro-metaphase I in mouse oocytes

(A) Live cell light-sheet imaging of WT and BC- MLN-treated KO oocytes during Early pro-metaphase I; aMTOC (gray), SiR-tubulin (green), DNA (magenta). Time is indicated in h:min; Scale bar 10 μm (B, D) Quantification of spindle volume over time in WT (B) and BC-KO (D), respectively.

(C, E) Quantification of area and aMTOC numbers over time in WT (C) and BC-KO (E), respectively. Yellow shadow: DMSO-treated; Purple shadow: MLN-treated. The red arrows indicate MLN addition time. Number of oocytes: WT DMSO: 11; WT MLN: 16; BC-KO DMSO:6; BC-KO MLN:8.

In particular, the level of expression of each individual AURKA fusion could be different from each other, altering the level of rescue that they perform. In this work, we use a concentration in which WT-AURKA rescues spindle defects and meiotic progression in oocytes where AURKA had been deleted.[20] These results were consistent with fixed oocyte phenotypes. Because the Chromatin-AURKA fusion appeared to increase in expression compared to WT and MTOC-AURKA, we evaluated the possibility of a dominant negative effect of this fusion by co-expressing WT-AURKA and Chromatin-AURKA in ABC-KO oocytes. Oocytes expressing both constructs showed similar spindle volumes to oocytes expressing only WT-AURKA (Figures 4L and 4M), suggesting that the failure of rescuing spindle defect by Chromatin-AURKA expression is not because of a dominant negative effect. This result is consistent with studies that evaluated H2B-targeted AURKA in mitotic cells.[26–28] Taken together, these results suggest that MTOC-localized AURKA is needed for normal spindle formation (Figure 5). Consistent with our results, when Pericentrin (aMTOC) is depleted via Trim-away,[29] mouse oocytes can build bipolar spindles relying mostly on the Ran-GTP pathway, similar to human oocytes. Notably, a previous study showed that Pericentrin-depleted spindles were shorter than controls.[1] The same results were observed in mouse oocytes when Pericentrin was conditionally knocked down, or when spindle pole structure was altered. In both scenarios, spindles were shorter.[24,30,31] The cellular context in our experiments is different because aMTOCs are present, but defective in structure. We speculate that their presence does not trigger the Ran-GTP backup pathway and therefore they function abnormally, producing defective spindles. Although human oocytes do not have aMTOCs, some of the components, including AURKA, are enriched at spindle poles suggesting some functional role.[14] However, the role of AURKA in spindle formation and stability in human oocytes requires further investigation.

Although the aMTOC-AURKA fusion was designed to localize to aMTOCs, we observed some signals at kinetochores (Figure 4D) where AURKC would normally localize. To resolve specific AURKA vs. AURKC functions, we genetically added back AURKC (Figures S3C and S3D) and evaluated spindle phenotypes in AB-KO oocytes expressing the MTOC-AURKA fusion. When MTOC-AURKA was overexpressed in AB-KO oocytes (AURKC only), we did not observe MTOC-AURKA at kinetochores (Figure S6A). We then compared the level of spindle rescue between AB-KO oocytes and ABC-KO oocytes overexpressing either WT-AURKA or MTOC-AURKA. Interestingly, there were no significant differences in TACC3 intensity between the genotypes, but there were differences between the AURKA fusion proteins (Figures S6A–S6C). In both genotypes, when oocytes overexpressed MTOC-AURKA, TACC3 intensity was reduced by 40% compared to controls. There were significant differences in spindle volume both between variants and between genotypes (Figures S6A–S6C). In AB-KO oocytes expressing MTOC-AURKA, spindle volume was reduced by 40% compared to controls. In ABC-KO oocytes, spindle volume was reduced by 50% when MTOC-AURKA was expressed. Although spindle volumes differed between genotypes, we observed that neither AB-KO nor ABC-KO oocytes expressing MTOC-AURKA had fully rescued spindle volumes and LISD organization. Taken together, these results suggest that AURKC does not regulate LISD formation but does contribute to a more significant rescue of spindle parameters (Figure 5).

DISCUSSION

In this study, we used a combination of genetic and pharmacological approaches to understand what steps of spindle assembly require AURKA and where in the oocyte AURKA carries out these steps. We find that MTOC-localized AURKA is required for normal spindle assembly and stability (Figure 5). Our data show that neither AURKA fusion fully rescue spindle formation. It is possible that the targeting does not allow for translocation or diffusion along the spindle. In somatic cells, a gradient of AURKA exists, extending from centrosomes to metaphase plates. This gradient is important for HEC1 phosphorylation at kinetochores,[32] which is critical for spindle elongation and spindle pole formation in mouse oocytes.[33] Therefore, whether Chromatin-AURKA can phosphorylate HEC1, or whether there is a third population of AURKA at kinetochores in oocytes requires further studies. An alternative explanation is that AURKA regulates additional processes that indirectly affect spindle formation. For example, in somatic cells, AURKA localizes to mitochondria,[34,35] and regulates mitochondrial dynamics and ATP production. Whether AURKA has the same role in oocytes is unknown. Another potential AURKA role in oocytes is regulating protein homeostasis. Fully grown oocytes are transcriptionally silent and regulated translation is critical.[36] In *Xenopus* oocytes, AURKA phosphorylates CPEB1, an inhibitor of translation. Phosphorylation of CPEB1 promotes its degradation and translation of maternal mRNA.[37] In mouse oocytes lacking *Aurka*, CPEB1 is not fully phosphorylated, and levels of total translation are reduced compared to WT.[38,39] Therefore, by targeting AURKA, we may interfere with AURKA localization to mitochondria or translation activation and affect oocyte energy and protein requirements.

Limitations of study

The approaches used in this study have some limitations. The use of chemical inhibitors such as MLN could have off targets effects. Although we used a concentration that was defined to specifically inhibit AURKA in mouse oocytes,[25] we cannot discard the possibility that we are affecting other pathways that could be also relevant during spindle assembly.

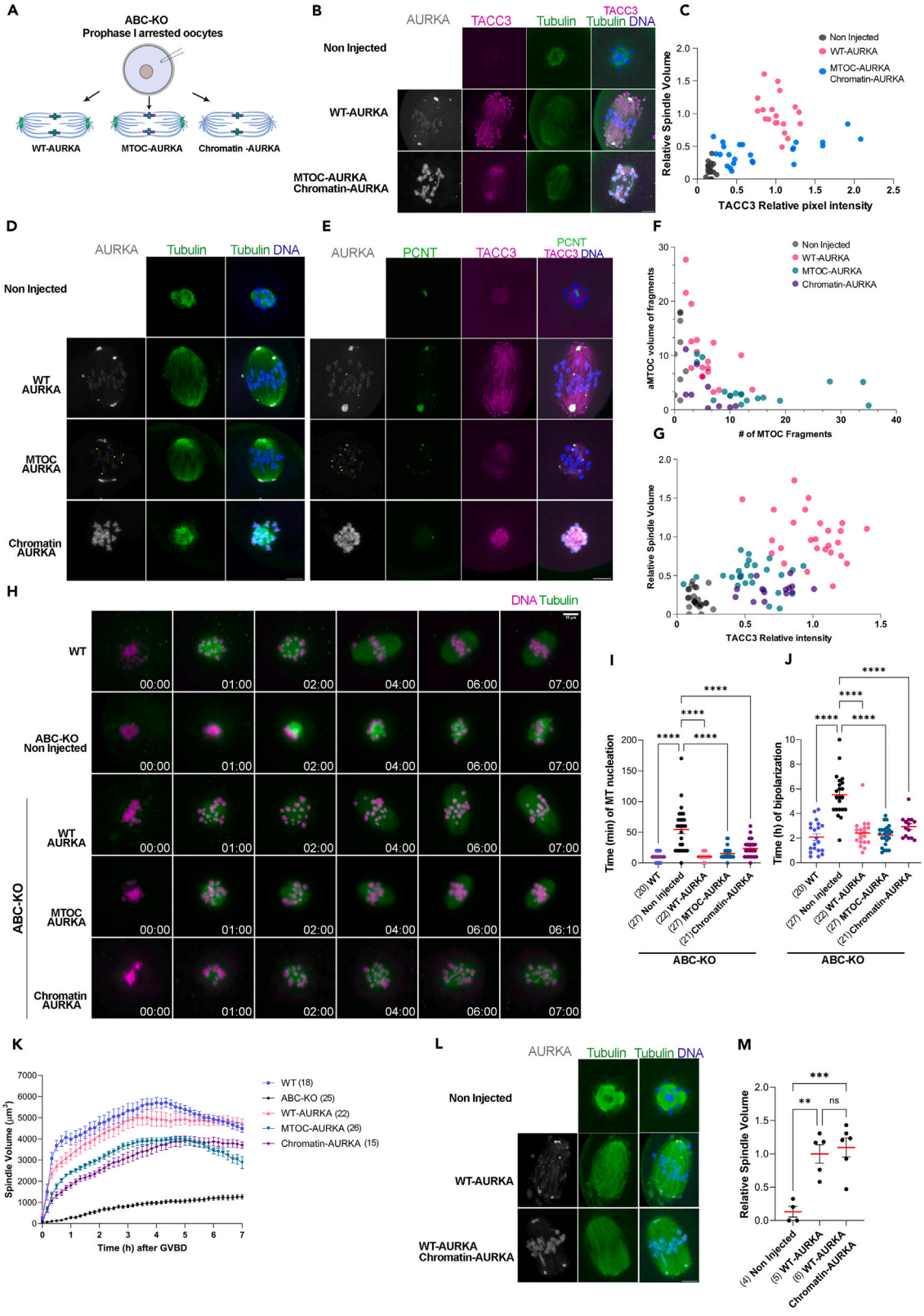
A
ABC-KO
Prophase I arrested oocytes
WT-AURKA
MTOC-AURKA
Chromatin -AURKA
B
AURKA
TACC3
Tubulin
TACC3
Tubulin DNA
Non Injected
WT-AURKA
MTOC-AURKA
Chromatin-AURKA
C
Non Injected
WT-AURKA
MTOC-AURKA
Chromatin-AURKA
Relative Spindle Volume
TACC3 Relative pixel intensity
D
AURKA
Tubulin
Tubulin DNA
Non Injected
WT AURKA
MTOC AURKA
Chromatin AURKA
E
AURKA
PCNT
TACC3
PCNT
TACC3 DNA
F
Non Injected
WT-AURKA
MTOC-AURKA
Chromatin-AURKA
aMTOC volume of fragments
# of MTOC Fragments
G
Relative Spindle Volume
TACC3 Relative intensity
H
DNA Tubulin
WT
ABC-KO Non Injected
ABC-KO
WT AURKA
MTOC AURKA
Chromatin AURKA
00:00
01:00
02:00
04:00
06:00
06:10
07:00
I
Time (min) of MT nucleation
(20) WT
(27) Non injected
(22) WT-AURKA
(27) MTOC-AURKA
(21) Chromatin-AURKA
ABC-KO
J
Time (h) of bipolarization
(20) WT
(27) Non injected
(22) WT-AURKA
(27) MTOC-AURKA
(21) Chromatin-AURKA
ABC-KO
K
Spindle Volume (µm³)
Time (h) after GVBD
WT (18)
ABC-KO (25)
WT-AURKA (22)
MTOC-AURKA (26)
Chromatin-AURKA (15)
L
AURKA
Tubulin
Tubulin DNA
Non Injected
WT-AURKA
WT-AURKA Chromatin-AURKA
M
Relative Spindle Volume
ns
(4) Non Injected
(5) WT-AURKA
(6) WT-AURKA Chromatin-AURKA

Figure 4. MTOC-AURKA partially rescued spindle phenotypes in ABC-KO oocytes

(A) Schematic of the experimental design. ABC-KO oocytes microinjected with different AURKA fusions. Localization of AURKA is green.

(B) Representative confocal images of Metaphase I ABC-KO oocytes expressing the indicated fusions. Non-injected ABC-KO oocytes were control. Oocytes were immunostained with TACC3 (magenta), tubulin (green), DAPI (blue). Localization of the targeted AURKA fusion is gray. Scale bar 10 μm.

(C) Quantification of spindle and LISD parameters in (B). Gray dots: Non-injected oocytes; pink dots: WT-AURKA; blue dots: MTOC-AURKA + chromatin-AURKA.

(D and E) Representative confocal images of Metaphase I ABC-KO oocytes expressing the indicated fusions immunostained with tubulin (green), DAPI (DNA) in (D) and PCNT (green), TACC3 (magenta), DAPI (DNA) in (E). Localization of the targeted AURKA fusion is gray. Scale bars: 5 μm.

(F) Quantification of aMTOC parameters.

(G) Quantification of spindle and LISD parameters. Gray dots: Non-injected oocytes; pink dots: WT-AURKA; green dots: MTOC-AURKA, and purple dots: chromatin-AURKA.

(H) Live cell light-sheet imaging of WT and ABC-KO oocytes. ABC-KO oocytes express the indicated fusion, Sir-tubulin (green), DNA (magenta). (I) Time of MT nucleation and (J) time of spindle bipolarization (One-way ANOVA, $****p < 0.0001$). Data are represented as mean ± SEM.

(K) Spindle volume during meiotic maturation. Time stamp (h:min) is relative to GVBD.

(L) Representative confocal image of ABC-KO oocytes from three mice at Metaphase I expressing the indicated Gfp fusions (gray). Oocytes were immunostained with tubulin (green) and DAPI (blue). Scale bar 10 μm.

(M) Quantification of spindle volume in (L). (One-way ANOVA, $**p < 0.001$; $***p < 0.001$; ns = not significant). In brackets are the number of oocytes analyzed in at least 3 independent experiments. See also Figure S3–S6.

In conclusion, we establish the temporal requirements of AURKA during spindle formation, determine that AURKA localized to aMTOCs is the major population required for spindle organization and suggest roles for AURKC in spindle building during late pro-metaphase I in mouse oocytes (Figure 5). This study raises new questions about non-canonical roles of AURKA during meiotic maturation that are important for understanding the mechanism that ensures oocyte quality that should be further examined.

STAR★METHODS

Detailed methods are provided in the online version of this paper and include the following:

- KEY RESOURCES TABLE
- RESOURCE AVAILABILITY
  - Lead contact
  - Materials availability
  - Data and code availability
- EXPERIMENTAL MODEL AND STUDY PARTICIPANT DETAILS
- METHOD DETAILS
  - Genotyping
  - Oocyte collection, maturation, and microinjection
  - Immunocytochemistry
  - Live imaging
  - Plasmid information
  - Drugs and antibodies
  - Microscopy
  - Image analysis
- QUANTIFICATION AND STATISTICAL ANALYSIS

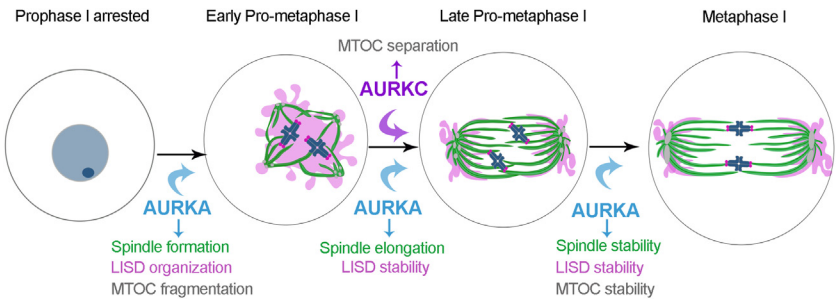

Figure 5. Model depicting AURKA and AURKC roles during spindle formation in mouse oocytes

At early pro-metaphase I, AURKA (light blue) is needed for aMTOC (gray) fragmentation, LISD (magenta) organization and spindle (green) formation; at late pro-metaphase I, AURKA is required for LISD stability and spindle elongation; whilst AURKC (purple) is needed for aMTOC separation. Finally at metaphase I, AURKA is required for aMTOC, LISD and spindle stability.

SUPPLEMENTAL INFORMATION

Supplemental information can be found online at https://doi.org/10.1016/j.isci.2024.110451.

ACKNOWLEDGMENTS

This work was funded by NIH grant R35 GM136340 to KS and Grant Agency of the Czech Republic grant 23-07532S to DD The authors acknowledge members of the Schindler lab and Devanshi Jain for helpful discussions.

AUTHOR CONTRIBUTIONS

Conceptualization, C.S.B and K.S.; experimental execution: C.S.B and M.V.; methodology, C.S.B., M.V., D.D., and J.S.; data analysis, C.S.B, M.V., D.D.; visualization, C.S.B.; writing original draft, C.S.B. and K.S.; review and editing article, C.S.B, M.V., J.S., D.D., and K.S.; funding, K.S and D.D.

DECLARATION OF INTERESTS

The authors declare no competing interests.

Received: April 3, 2024
Revised: May 30, 2024
Accepted: July 1, 2024
Published: July 3, 2024

REFERENCES

1. So, C., Menelaou, K., Uraji, J., Harasimov, K., Steyer, A.M., Seres, K.B., Bucevičius, J., Lukinavičius, G., Möbius, W., Sibold, C., et al. (2022). Mechanism of spindle pole organization and instability in human oocytes. Science *375*, eabj3944. https://doi.org/10.1126/science.abj3944.
2. Schatten, H., and Sun, Q.Y. (2015). Centrosome and microtubule functions and dysfunctions in meiosis: implications for age-related infertility and developmental disorders. Reprod. Fertil. Dev. *27*, 934–943. https://doi.org/10.1071/RD14493.
3. Manandhar, G., Schatten, H., and Sutovsky, P. (2005). Centrosome reduction during gametogenesis and its significance. Biol. Reprod. *72*, 2–13. https://doi.org/10.1095/biolreprod.104.031245.
4. Holubcová, Z., Blayney, M., Elder, K., and Schuh, M. (2015). Human oocytes. Error-prone chromosome-mediated spindle assembly favors chromosome segregation defects in human oocytes. Science (New York, N.Y.) *348*, 1143–1147. https://doi.org/10.1126/science.aaa9529.
5. Schuh, M., and Ellenberg, J. (2007). Self-organization of MTOCs replaces centrosome function during acentrosomal spindle assembly in live mouse oocytes. Cell *130*, 484–498. https://doi.org/10.1016/j.cell.2007.06.025.
6. Dumont, J., Petri, S., Pellegrin, F., Terret, M.E., Bohnsack, M.T., Rassinier, P., Georget, V., Kalab, P., Gruss, O.J., and Verlhac, M.H. (2007). A centriole- and RanGTP-independent spindle assembly pathway in meiosis I of vertebrate oocytes. J. Cell Biol. *176*, 295–305. https://doi.org/10.1083/jcb.200605199.
7. Drutovic, D., Duan, X., Li, R., Kalab, P., and Solc, P. (2020). RanGTP and importin beta regulate meiosis I spindle assembly and function in mouse oocytes. EMBO J. *39*, e101689. https://doi.org/10.15252/embj.2019101689.
8. Combelles, C.M., and Albertini, D.F. (2001). Microtubule patterning during meiotic maturation in mouse oocytes is determined by cell cycle-specific sorting and redistribution of gamma-tubulin. Dev. Biol. *239*, 281–294. https://doi.org/10.1006/dbio.2001.0444.
9. Ma, W., and Viveiros, M.M. (2014). Depletion of pericentrin in mouse oocytes disrupts microtubule organizing center function and meiotic spindle organization. Mol. Reprod. Dev. *81*, 1019–1029. https://doi.org/10.1002/mrd.22422.
10. Brunet, S., Dumont, J., Lee, K.W., Kinoshita, K., Hikal, P., Gruss, O.J., Maro, B., and Verlhac, M.H. (2008). Meiotic regulation of TPX2 protein levels governs cell cycle progression in mouse oocytes. PLoS One *3*, e3338. https://doi.org/10.1371/journal.pone.0003338.
11. Megraw, T.L., and Kaufman, T.C. (1999). The centrosome in Drosophila oocyte development. In Current Topics in Developmental Biology, R.E. Palazzo and G.P. Schatten, eds. (Academic Press), pp. 385–407. https://doi.org/10.1016/S0070-2153(99)49019-2.
12. Clift, D., and Schuh, M. (2015). A three-step MTOC fragmentation mechanism facilitates bipolar spindle assembly in mouse oocytes. Nat. Commun. *6*, 7217. https://doi.org/10.1038/ncomms8217.
13. Tyc, K.M., El Yakoubi, W., Bag, A., Landis, J., Zhan, Y., Treff, N.R., Scott, R.T., Jr., Tao, X., Schindler, K., and Xing, J. (2020). Exome sequencing links CEP120 mutation to maternally derived aneuploid conception risk. Hum. Reprod. *35*, 2134–2148. https://doi.org/10.1093/humrep/deaa148.
14. Wu, T., Dong, J., Fu, J., Kuang, Y., Chen, B., Gu, H., Luo, Y., Gu, R., Zhang, M., Li, W., et al. (2022). The mechanism of acentrosomal spindle assembly in human oocytes. Science *378*, eabq7361. https://doi.org/10.1126/science.abq7361.
15. So, C., Seres, K.B., Steyer, A.M., Monnich, E., Clift, D., Pejkovska, A., Mobius, W., and Schuh, M. (2019). A liquid-like spindle domain promotes acentrosomal spindle assembly in mammalian oocytes. Science *364*, eaat9557. https://doi.org/10.1126/science.aat9557.
16. Shuda, K., Schindler, K., Ma, J., Schultz, R.M., and Donovan, P.J. (2009). Aurora kinase B modulates chromosome alignment in mouse oocytes. Mol. Reprod. Dev. *76*, 1094–1105. https://doi.org/10.1002/mrd.21075.
17. Ding, J., Swain, J.E., and Smith, G.D. (2011). Aurora kinase-A regulates microtubule organizing center (MTOC) localization, chromosome dynamics, and histone-H3 phosphorylation in mouse oocytes. Mol. Reprod. Dev. *78*, 80–90. https://doi.org/10.1002/mrd.21272.
18. Kratka, C., Drutovic, D., Blengini, C.S., and Schindler, K. (2022). Using ZINC08918027 inhibitor to determine Aurora kinase-chromosomal passenger complex isoforms in mouse oocytes. BMC Res. Notes *15*, 96. https://doi.org/10.1186/s13104-022-05987-4.
19. Balboula, A.Z., Nguyen, A.L., Gentilello, A.S., Quartuccio, S.M., Drutovic, D., Solc, P., and Schindler, K. (2016). Haspin kinase regulates microtubule-organizing center clustering and stability through Aurora kinase C in mouse oocytes. J. Cell Sci. *129*, 3648–3660. https://doi.org/10.1242/jcs.189340.
20. Blengini, C.S., Ibrahimian, P., Vaskovicova, M., Drutovic, D., Solc, P., and Schindler, K. (2021). Aurora kinase A is essential for meiosis in mouse oocytes. PLoS Genet. *17*, e1009327. https://doi.org/10.1371/journal.pgen.1009327.
21. Nguyen, A.L., Drutovic, D., Vazquez, B.N., El Yakoubi, W., Gentilello, A.S., Malumbres, M., Solc, P., and Schindler, K. (2018). Genetic Interactions between the Aurora Kinases Reveal New Requirements for AURKB and AURKC during Oocyte Meiosis. Curr. Biol. *28*, 3458–3468.e5. https://doi.org/10.1016/j.cub.2018.08.052.
22. Schindler, K., Davydenko, O., Fram, B., Lampson, M.A., and Schultz, R.M. (2012). Maternally recruited Aurora C kinase is more stable than Aurora B to support mouse oocyte maturation and early development.

Proc. Natl. Acad. Sci. USA *109*, E2215–E2222. https://doi.org/10.1073/pnas.1120517109.
23. Solc, P., Baran, V., Mayer, A., Bohmova, T., Panenkova-Havlova, G., Saskova, A., Schultz, R.M., and Motlik, J. (2012). Aurora kinase A drives MTOC biogenesis but does not trigger resumption of meiosis in mouse oocytes matured in vivo. Biol. Reprod. *87*, 85. https://doi.org/10.1095/biolreprod.112.101014.
24. Wang, X., Baumann, C., De La Fuente, R., and Viveiros, M.M. (2020). CEP215 and AURKA regulate spindle pole focusing and aMTOC organization in mouse oocytes. Reproduction *159*, 261–274. https://doi.org/10.1530/REP-19-0263.
25. Blengini, C.S., Ik Jung, G., Aboelenain, M., and Schindler, K. (2022). A field guide to Aurora kinase inhibitors: an oocyte perspective. Reproduction *164*, V5–V7. https://doi.org/10.1530/rep-22-0292.
26. Li, S., Deng, Z., Fu, J., Xu, C., Xin, G., Wu, Z., Luo, J., Wang, G., Zhang, S., Zhang, B., et al. (2015). Spatial Compartmentalization Specializes the Function of Aurora A and Aurora B. J. Biol. Chem. *290*, 17546–17558. https://doi.org/10.1074/jbc.M115.652453.
27. Wang, E., Ballister, E.R., and Lampson, M.A. (2011). Aurora B dynamics at centromeres create a diffusion-based phosphorylation gradient. J. Cell Biol. *194*, 539–549. https://doi.org/10.1083/jcb.201103044.
28. Pfisterer, M., Robert, R., Saul, V.V., Pritz, A., Seibert, M., Feederle, R., and Schmitz, M.L. (2024). The Aurora B-controlled PP1/RepoMan complex determines the spatial and temporal distribution of mitotic H2B S6 phosphorylation. Open Biol. *14*, 230460. https://doi.org/10.1098/rsob.230460.
29. Clift, D., McEwan, W.A., Labzin, L.I., Konieczny, V., Mogessie, B., James, L.C., and Schuh, M. (2017). A Method for the Acute and Rapid Degradation of Endogenous Proteins. Cell *171*, 1692–1706.e18. https://doi.org/10.1016/j.cell.2017.10.033.
30. Baumann, C., Wang, X., Yang, L., and Viveiros, M.M. (2017). Error-prone meiotic division and subfertility in mice with oocyte-conditional knockdown of pericentrin. J. Cell Sci. *130*, 1251–1262. https://doi.org/10.1242/jcs.196188.
31. Wang, X., Baumann, C., De La Fuente, R., and Viveiros, M.M. (2021). Loss of acentriolar MTOCs disrupts spindle pole Aurora A and assembly of the liquid-like meiotic spindle domain in oocytes. J. Cell Sci. *134*, jcs256297. https://doi.org/10.1242/jcs.256297.
32. Iemura, K., Natsume, T., Maehara, K., Kanemaki, M.T., and Tanaka, K. (2021). Chromosome oscillation promotes Aurora A-dependent Hec1 phosphorylation and mitotic fidelity. J. Cell Biol. *220*, e202006116. https://doi.org/10.1083/jcb.202006116.
33. Courtois, A., Yoshida, S., Takenouchi, O., Asai, K., and Kitajima, T.S. (2021). Stable kinetochore–microtubule attachments restrict MTOC position and spindle elongation in oocytes. EMBO Rep. *22*, e51400. https://doi.org/10.15252/embr.202051400.
34. Grant, R., Abdelbaki, A., Bertoldi, A., Gavilan, M.P., Mansfeld, J., Glover, D.M., and Lindon, C. (2018). Constitutive regulation of mitochondrial morphology by Aurora A kinase depends on a predicted cryptic targeting sequence at the N-terminus. Open Biol. *8*, 170272. https://doi.org/10.1098/rsob.170272.
35. Bertolin, G., Bulteau, A.L., Alves-Guerra, M.C., Burel, A., Lavault, M.T., Gavard, O., Le Bras, S., Gagné, J.P., Poirier, G.G., Le Borgne, R., et al. (2018). Aurora kinase A localises to mitochondria to control organelle dynamics and energy production. Elife *7*, e38111. https://doi.org/10.7554/eLife.38111.
36. Richter, J.D., and Lasko, P. (2011). Translational control in oocyte development. Cold Spring Harb. Perspect. Biol. *3*, a002758. https://doi.org/10.1101/cshperspect.a002758.
37. Han, S.J., Martins, J.P.S., Yang, Y., Kang, M.K., Daldello, E.M., and Conti, M. (2017). The Translation of Cyclin B1 and B2 is Differentially Regulated during Mouse Oocyte Reentry into the Meiotic Cell Cycle. Sci. Rep. *7*, 14077. https://doi.org/10.1038/s41598-017-13688-3.
38. Aboelenain, M., and Schindler, K. (2021). Aurora kinase B inhibits aurora kinase A to control maternal mRNA translation in mouse oocytes. Development *148*, dev199560. https://doi.org/10.1242/dev.199560.
39. Kunitomi, C., Romero, M., Daldello, E.M., Schindler, K., and Conti, M. (2024). Multiple intersecting pathways are involved in the phosphorylation of CPEB1 to activate translation during mouse oocyte meiosis. Preprint at bioRxiv. https://doi.org/10.1101/2024.01.17.575938.
40. Kitajima, T.S., Ohsugi, M., and Ellenberg, J. (2011). Complete kinetochore tracking reveals error-prone homologous chromosome biorientation in mammalian oocytes. Cell *146*, 568–581. https://doi.org/10.1016/j.cell.2011.07.031.
41. Blengini, C.S., and Schindler, K. (2018). Immunofluorescence Technique to Detect Subcellular Structures Critical to Oocyte Maturation. Methods Mol. Biol. *1818*, 67–76. https://doi.org/10.1007/978-1-4939-8603-3_8.
42. Wang, Z., Wu, T., Shi, L., Zhang, L., Zheng, W., Qu, J.Y., Niu, R., and Qi, R.Z. (2010). Conserved motif of CDK5RAP2 mediates its localization to centrosomes and the Golgi complex. J. Biol. Chem. *285*, 22658–22665. https://doi.org/10.1074/jbc.M110.105965.
43. Ferencova, I., Vaskovicova, M., Drutovic, D., Knoblochova, L., Macurek, L., Schultz, R.M., and Solc, P. (2022). CDC25B is required for the metaphase I-metaphase II transition in mouse oocytes. J. Cell Sci. *135*, jcs252924. https://doi.org/10.1242/jcs.252924.
44. Schindelin, J., Arganda-Carreras, I., Frise, E., Kaynig, V., Longair, M., Pietzsch, T., Preibisch, S., Rueden, C., Saalfeld, S., Schmid, B., et al. (2012). Fiji: an open-source platform for biological-image analysis. Nat. Methods *9*, 676–682. https://doi.org/10.1038/nmeth.2019.
45. Milletari, F., Navab, N., and Ahmadi, S.A. (2016). V-net: Fully Convolutional Neural Networks for Volumetric Medical Image Segmentation (Fourth International Conference on 3D Vision), pp. 565–571.

STAR★METHODS

KEY RESOURCES TABLE

REAGENT or RESOURCE	SOURCE	IDENTIFIER
Antibodies		
Mouse monoclonal Pericentrin antibody	BD Biosciences	Cat#611814; RRID: AB_399294
Rabbit TACC3 antibody	Novus Biologicals	Cat# NBP2-67671
Sheep polyclonal Alpha Tubulin antibody	Cytoskeleton	Cat#ATN02; RRID: AB_10708807
Rabbit phosphorylated Aurora A (Thr288), Aurora B (Thr232), Aurora C (Thr198) (D13A11) antibody	Cell Signaling Technology	Cat#2914; RRID: AB_2061631
Rabbit phosphorylated CDC25B (Ser323) antibody	Signalway Antibodies	Cat#11949
phosphorylated INCENP	Gift from Dr. Michael Lampson	Not applicable
Donkey anti-mouse Alexa Fluor 568 Secondary antibody	Life Technologies	Cat#A10037; RRID: AB_11180865
Donkey anti-rabbit Alexa Fluor 647 Secondary antibody	Life Technologies	Cat#A31573; RRID: AB_2536183
Anti-sheep-Alexa-488 Secondary antibody	Life Technologies	Cat#A11015; RRID: AB_2534082
Human polyclonal anti-centromere protein antibody	Antibodies Incorporated	Cat# 15–235; RRID: AB_2939059
Chemicals, peptides, and recombinant proteins		
Pregnant Mare Serum Gonadotropin (PMSG)	Calbiochem Lee-Biosolutions	Cat#367222 Cat#493-10
Milrinone	Sigma-Aldrich	Cat#M4659
MLN8237 (Alisertib)	Selleck Chemicals	Cat#S1133
MG132	Selleck Chemicals	Cat#S2619
Dimethyl sulfoxide (DMSO	Sigma-Aldrich	Cat#472301
Bovine Serum Albumin (BSA)	Sigma-Aldrich	Cat#A4503; Cat#A3311
SiR-tubulin	Spirochrome	Cat#SC002
SiR-DNA	Spirochrome	Cat#SC007
DAPI	Life Technologies	Cat#D1306
Vectashield	Vector Laboratories	Cat#H-1000
L-glutamine	GIBCO	Cat#25030-08
Paraformaldehyde	Sigma-Aldrich	Cat#P6148
CZB culture Media		
MEM culture Media	Sigma-Aldrich	Cat#M4655
M2 media	Sigma-Aldrich	Cat#M7167
penicillin–streptomycin	Merck	Cat#P7794, #S1277
Mineral oil	Sigma-Aldrich	Cat#M5310
Sodium pyruvate	Sigma-Aldrich	Cat#P4562
Critical commercial assays		
mMESSAGE machine T3	Ambion, Thermo Fisher Scientific	Cat#AM1348
Poly(A) Tailing Kit	Ambion, Thermo Fisher Scientific	Cat#AM1350
RNeasy Mini Kit	QIAGEN	Cat#74104
Experimental models: Organisms/strains		
Mouse: A-KO	Blengini et al.[20]	
Mouse: BC-KO	Nguyen et al.[21]	
Mouse: AB-KO	This paper	
Mouse: ABC-KO	This paper	

(*Continued on next page*)

Continued

REAGENT or RESOURCE	SOURCE	IDENTIFIER
Recombinant DNA		
Aurka-Gfp	Nguyen et al.[21]	
Aurka-Eyfp	Blengini et al.[20]	
CDK5RAP fr-Aurka-Eyfp	This paper	
H2B-Aurka-Eyfp	This paper	
Egfp-Cdk5rap2	Balboula et al.[19]	
H2b-mCherry	Kitajima et al.[40]	
Software and algorithms		
Fiji	National Institute of Health	https://fiji.sc/
Imaris	Oxford instruments	https://imaris.oxinst.com/
Convolutional Neural Network based on the V-net architecture	Milletari et al.	
Prism 10	Graphpad	https://www.graphpad.com/

RESOURCE AVAILABILITY

Lead contact

Information and requests for resources and reagents should be directed to and will be fulfilled by the lead contact, Karen Schindler (Ks804@hginj.rutgers.edu).

Materials availability

Plasmids generated in this study are available without restriction from the lead contact, Karen Schindler. *Aurka* and *Aurkb* conditional knockout mice are available without restriction from the lead contact. *Aurkc* knockout mice were purchased from Taconic and under an MTA license.

Data and code availability

- All data reported in this paper is available from the lead contact upon request.
- This paper does not report original code.
- Any additional information required to reanalyze the data reported in this paper is available from the lead contact upon request.

EXPERIMENTAL MODEL AND STUDY PARTICIPANT DETAILS

The different strains of mice used in this work were generated by mating of floxed *Aurka* (C57BL/6N) (Aurka$^{f/f}$) mice or *Aurkb*$^{fl/fl}$ Gdf9-Cre mice with double knockout mice for AURKB and AURKC (C57BL/6J, 129/Sv) (*Aurkb*$^{f/f}$, *Aurkc*$^{-/-}$, Gdf9-Cre mice (BC-KO), described before.[20–22] After several rounds of mating, we isolated animals that were *Aurka*$^{f/f}$, *Aurkb*$^{f/f}$, and Gdf9-Cre mice (AB-KO), and Gdf9-Cre mice (ABC-KO). Moreover, we also used animals *Aurkb*$^{f/f}$, *Aurkc*$^{-/-}$, and Gdf9-Cre mice (BC-KO). Control animals (Wild-type (WT)) were *Aurka*$^{f/f}$, and *Aurkb*$^{f/f}$ but lacking the Cre recombinase transgene. Mice were housed on a 12–12 h light-dark cycle, with constant temperature and with food and water were provided *ad libitum*. Animals were maintained in accordance with guidelines of the Institutional Animal Use and Care Committee of Rutgers University (protocol 201702497), the guidelines of National Institutes of Health guidelines, and the policies of the Expert Committee for the Approval of Projects of Experiments on Animals of the Academy of Sciences of the Czech Republic (protocol 106/2020). These regulatory bodies approved all experimental procedures involving the animals. All oocyte experiments were conducted using healthy female mice aged 6–16 weeks. Genotyping was performed before weaning and repeated when the animals were used for experiments as previously described.[20,21]

METHOD DETAILS

Genotyping

Genotyping was performed before weaning and repeated upon use of the animals for experiments for replication and confirmation. *LoxP* and Cre genotyping was performed by PCR amplification. Primers for *Aurka LoxP* (Forward: 5′-CTGGATCACAGGTGTGGAGT-3′, Reverse: 5′-GGCTACATGCAGGCAAACA-3′),

Aurkb LoxP (Forward: 5′-AGGGCCTAATTGCCTCTTGT-3′, Reverse: 5′-GGGCATGAATTCTTGAGTCG-3′), and *Gdf9-Cre* (Forward: 5′-GGCATGCTTGAGGTCTGATTAC-3′, Reverse: 5′-CAGGTTTTGGTGCACAGTCA-3′, Internal control Forward: 5′-CTAGGCCACAGAATT-GAAAGATCT-3′, Internal control Reverse: 5′-GTAGGTGGAAATTCTAGCATCATCC-3′). Primers were used at a final concentration of

1 μM, and Taq 2xMaster Mix (NEB, #M0270L) was used following the manufacturer's protocol. The sizes of products were for *Aurka*: 243 bp for WT and 372 bp for lox/lox transgene; for *Aurkb*: 350 bp for WT and 500 bp for lox/lox transgene, for Cre: 324 bp for no Cre and 200 bp + 324 bp for Cre presence. Deletion of AURKC was detected by a TaqMan copy number assay using primers/probes to detect *Neo* (Assay #Mr00299300_cn) and Tfrc (for normalization; Assay #4458366). The delta-delta Ct method was used to determine expression levels. PCR conditions are available on request.

Oocyte collection, maturation, and microinjection

Prophase I-arrested oocytes were collected from ovaries of of 6–16 weeks old females injected 48 h earlier with 5 I.U. of pregnant mare's serum gonadotropin (PMSG) (Lee Biosolutions #493–10). Oocytes were collected as described previously.[41] Briefly, ovaries were placed in minimal essential medium (MEM) containing 2.5 μM milrinone (Sigma-Aldrich #M4659) to prevent meiotic resumption and oocytes were isolated by piercing the ovaries with needles. To induce meiotic resumption, oocytes were cultured in milrinone-free Chatot, Ziomek, and Bavister (CZB) medium in an atmosphere of 5% CO_2 in air at 37°C. Oocytes were matured for different periods depending on the experimental conditions: to reach early prometaphase I, 3 h after milrinone wash; for late prometaphase I, 5 h after milrinone wash; for metaphase I, 7–7.5 h after milrinone wash, and to evaluate spindle stability we matured the oocytes for 10 h after milrinone wash.

For microinjection, prophase-arrested oocytes were maintained in CZB supplemented with 2.5 μM milrinone to keep them arrested. Oocytes were microinjected with 100 ng/μL Aurka-Gfp (WT AURKA), 100 ng/μL H2B-Aurka-Eyfp (Chromatin- AURKA), 100 ng/μL CDK5FRAP fr-Aurka-Eyfp (MTOC-AURKA), or with 100 ng/μL H2B-Aurka-Eyfp and 100 ng/μL CDK5FRAP fr-Aurka-Eyfp *together. Microinjected oocytes were cultured overnight in* CZB supplemented with 2.5 μM milrinone to allow protein expression prior to the procedures. Subsequently, the oocytes were allowed to mature for 7–7.5 h to reach metaphase I.

For light-sheet live cell imaging, oocytes were microinjected in M2 medium with ~10 pL of 50 ng/μL *H2b-mCherry*, 10 ng/μL of *Aurka-Eyfp*, *Aurka*, *H2b-Aurka-Eyfp* and *Aurka-Cdk5rap2-Eyfp*, 100–150 ng/μL *Egfp-Cdk5rap2*, and 75 nM SiR-DNA (Spirochrome, #SC007) or SiR-tubulin (Spirochrome, #SC002) was used for staining chromosomes and spindle, respectively. For protein expression, oocytes were incubated in culture medium supplemented with milrinone for 3 h after microinjection.

Immunocytochemistry

After maturation oocytes were immunostained according to a previously described protocol.[41] Briefly, oocytes were fixed in phosphate buffer saline (PBS) containing paraformaldehyde (PFA) 2% for 20 min at room temperature. Oocytes were then incubated in permeabilization solution (PBS containing 0.1% (v/v) Triton X-100 and 0.3% (w/v) BSA) for 20 min, followed by 10 min in blocking buffer (0.3% BSA containing 0.01% Tween in PBS). Immunostaining was performed by incubating cells in primary antibody overnight in a dark, humidified chamber at 4°C followed by 3 consecutive 10-min incubations in a blocking buffer. After washing, secondary antibodies were diluted 1:200 in blocking solution and the sample was incubated for 1 h at room temperature. After washing, the cells were mounted in 10 μL VectaShield (Vector Laboratories, #H-1000) with 4′, 6- Diamidino-2-Phenylindole, Dihydrochloride (DAPI; Life Technologies #D1306; 1:170).

Live imaging

Oocytes were collected and microinjected in M2 medium (Sigma-Aldrich, #M7167-50ML) containing 2.5 μM milrinone (Sigma-Aldrich) to prevent meiotic maturation. Oocytes were cultured in minimum essential medium (MEM, Merck, #M4655) containing 1.14 mM sodium pyruvate (Merck, #P4562), 4 mg/mL bovine serum albumin (BSA, Merck, #A3311), penicillin–streptomycin (75 U/mL-60 mg/mL, Merck, #P7794, #S1277). Culture and live imaging were performed at 37°C in a 5% CO^2 atmosphere.

Plasmid information

Preparation of pYX-EYFP plasmid was described previously (Blengini, 2021). *AURKA* coding sequence was cloned by PCR into pYX-EYFP to create pYX-AURKA-EYFP plasmid. H2B was cloned using NheI restriction sites into pYX-AURKA-EYFP to create pYX-H2B-AURKA-EYFP plasmid. mCDK5RAP2-MBD (amino acids His 1655 – Ser 1822, (NM_145990.4) was cloned into pYX-AURKA-EYFP plasmid by PCR to create pYX-AURKA-EYFP-CDK5RAP2-MBD (original plasmid pGEMHE-mEGFP-mCDK5RAP2 was a gift from Dr. Tomoya Kitajima.[40] CDK5RAP2-MBD fragment corresponds to the microtubule-binding domain (MBD) from human CDK5RAP2.[42]

For *in vitro* transcription, we used a mMESSAGE machine T3 (Ambion, Thermo Fisher Scientific, #AM1348). For polyadenylation of all mRNAs except H2B-mCherry, we used Poly(A) Tailing Kit (Ambion, Thermo Fisher Scientific, #AM1350). All mRNAs were purified using RNeasy Mini Kit (QIAGEN, #74104) and stored at −80°C.

Drugs and antibodies

Based on a previous study where different Aurora kinase inhibitors were tested in mouse oocytes, to inhibit AURKA, we chose MLN8237[25] (Alisertib, Selleckchem #S1133). MLN was added to CZB culture media at a final concentration of 1 μM. To avoid the entrance to anaphase I, we inhibited the proteasome by adding 5μM MG132 (Selleck Chemicals, #S2619) to the culture media.

Primary antibodies and concentrations were used as follows: Pericentrin (Pcnt) (mouse, 1:100; BD Biosciences, #611814); TACC3 (Rabbit, 1:100; Novus Biologicals # NBP2-67671), Alpha Tubulin polyclonal (Sheep, 1:100; Cytoskeleton #ATN02); phosphorylated ABC (rabbit, 1:100; Cell Signaling Technology, #2914), phosphorylated CDC25B (1:100; Signalway Antibodies #11949); phosphorylated INCENP (Gift from

Michael Lampson), Human anti-ACA (1:30, Antibodies Incorporated #15–234). Secondary antibodies were used at 1:200 for IF experiments: anti-mouse-Alexa-568 (Life Technologies #A10037), anti-rabbit-Alexa-647 (Life Technologies #A31573) and Anti-sheep-Alexa-488 (Life Technologies #A11015)

Microscopy

For fixed cells, images were captured using a Leica SP8 confocal microscope equipped with 40X. 1.30 NA oil immersion objective. Optical Z-stacks of 1.0 μm step with a zoom of 4.0. In those experiments where pixel intensity was compared, the laser power was kept constant among genotypes or treatments.

For live-cell imaging, oocytes were scanned using the Viventis LS1 Live light-sheet microscope system (Viventis Microscopy Sarl, Switzerland) with a Nikon 25X NA 1.1 detection objective with 1.5× zoom, as described previously.[43] Thirty-one 2-μm optical sections were taken with a 750x750-pixel image resolution using 10-min intervals. mClover/EGFP, EYFP, mCherry, and SiR fluorescence were excited by 488, 515, 561, and 638 nm laser lines. To detect mClover/EGFP and EYFP emissions, band-pass filters 525/50 and 539/30 were used. mCherry and SiR emissions were detected using a triple band-pass filter 488/561/640.

Image analysis

For analysis of TACC3 pixel intensity in fixed oocytes Fiji software[44] was used. We did a maximal projection of the z stack and we defined the region of interest around the spindle using a free-handed drawing tool, finally, we measured TACC3 intensity in that region of interest using the measurement tool. The volume of spindle and aMTOC fragments in fixed images was performed using Imaris software (Bitplane).

For the videos, image analysis was performed using Fiji software.[44] For basic analysis of meiotic maturation, missegregation, misalignment, MTOC, and spindle bi-polarization max projection from each oocyte was created. For spindle segmentation, we have used a Convolutional Neural Network based on the V-net architecture.[45] The training set consisted of data from 6 experimental datasets, containing between 6 and 20 positions. The annotations were obtained with Fiji, using Gaussian smoothing, followed by constant threshold segmentation and a manual cleanup of the annotation.

QUANTIFICATION AND STATISTICAL ANALYSIS

All experiments were conducted 3 times, any exception would be clarified in the figure legend. Student T-test, ANOVA one-way or two-way analysis were used to evaluate significant differences between/among groups, using Prism software (GraphPad software). Data is shown as the mean ± standard error of the mean (SEM).